


Fractional dynamics using an ensemble of classical trajectories

Zhaopeng Sun (孙兆鹏),^{1,2} Hao Dong (董昊),¹ and Yujun Zheng (郑雨军)^{1,*}

¹*School of Physics, Shandong University, Jinan 250100, China*

²*School of Physics and Optoelectronic Engineering, Ludong University, Yantai 264025, China*

 (Received 25 September 2017; revised manuscript received 31 December 2017; published 22 January 2018)

A trajectory-based formulation for fractional dynamics is presented and the trajectories are generated deterministically. In this theoretical framework, we derive a new class of estimators in terms of confluent hypergeometric function (${}_1F_1$) to represent the Riesz fractional derivative. Using this method, the simulation of free and confined Lévy flight are in excellent agreement with the exact numerical and analytical results. In addition, the barrier crossing in a bistable potential driven by Lévy noise of index α is investigated. In phase space, the behavior of trajectories reveal the feature of Lévy flight in a better perspective.

DOI: [10.1103/PhysRevE.97.012132](https://doi.org/10.1103/PhysRevE.97.012132)

I. INTRODUCTION

Anomalous diffusion has been attracting growing attention in some fields of modern science. The identification of anomalous diffusion is usually determined by mean square displacement of the form $\langle x^2 \rangle \sim t^\mu$, where $0 < \mu < 1$ is subdiffusion and $1 < \mu \leq 2$ is superdiffusion. Several frameworks, such as the continuous time random walk scheme [1–3], Brownian motion in a logarithmic potential [4,5], fractional Brownian motion [6], fractional Fokker-Planck equation (FFPE), and so on [7–10] have been established to describe anomalous diffusion. Anomalous diffusions tend to violate the central limit theorem of probability theory and can be achieved either by correlations or by long-tailed statistics. A case in point is the so-called Lévy flight which has been introduced in connection with superdiffusion.

The Lévy flight, as one of the important fractional process, has been used to model a variety of process, such as the diffusion of micelles in salted water [11], single-ion motion in a one-dimensional optical lattice [12], special problems in reaction dynamics [13], and even in animal movement [14,15]. It is a Markov process that can be characterized by the occurrence of a long jump. In particular, the corresponding probability density function (PDF) could have a heavier tail than the Gaussian density and its correlation function decays to zero much slower than the usual exponential rate. These features are responsible for the anomalous characteristics in the diffusion processes. A class of FFPE has been successfully employed to describe particles undergoing Lévy flight, and explain the development of anomalous dispersion. When the one-dimensional diffusion dynamics is under the influence of an external potential $U(x)$ with a white Lévy noise, the FFPE can be written as [16–18]

$$\frac{\partial W(x,t)}{\partial t} = \frac{\partial}{\partial x} [U'(x)W(x,t)] + DD_x^\alpha W(x,t), \quad (1)$$

where D denotes the generalized diffusion coefficient and relates to the intensity of Lévy noise, $U'(x) = \frac{\partial U(x)}{\partial x}$.

$\mathcal{D}_q^\alpha \equiv \frac{\partial^\alpha}{\partial |q|^\alpha}$ is the Riesz fractional derivative. For $1 < \alpha \leq 2$, the Riesz fractional derivative \mathcal{D}_q^α is defined as [19]

$$\mathcal{D}_q^\alpha f(q,t) = -\frac{1}{2\cos(\alpha\pi/2)\Gamma(2-\alpha)} \times \frac{\partial^2}{\partial q^2} \int_{-\infty}^{\infty} |q-q'|^{1-\alpha} f(q',t) dq', \quad (2)$$

however, for $\alpha = 1$ it is related to the Hilbert transform, namely,

$$\mathcal{D}_q^1 f(q,t) = -\frac{1}{\pi} \frac{\partial}{\partial q} \int_{-\infty}^{\infty} \frac{f(q',t) dq'}{q-q'}. \quad (3)$$

Such forms can ensure that jump lengths have a symmetric probability distribution. In addition, the Riesz fractional derivative can be understood through its Fourier transform [20]

$$\mathcal{D}_q^\alpha f(q,t) = -\frac{1}{2\pi} \int_{-\infty}^{\infty} f(k,t) \exp(-ikq) |k|^\alpha dk. \quad (4)$$

It is found that the Lévy flight plays important roles in physical, chemical, and biological fields. To explore the dynamic and stationary behaviors of the Lévy process, many methods for solving FFPE of Eq. (1) and its derivatives, such as the fractional Klein-Kramers equation [21], have been developed. For example, the finite difference method [22,23], finite volume method [24,25], and fast Fourier transform (FFT) method [26], and so on have been developed to discretize the Riesz fractional derivatives to solve the FFPE numerically. The realization of these methods need complicated numerical algorithms, which are usually abstract in describing the physical picture of the Lévy flight process.

In recent years many methods for propagating the (quantum) system by employing the evolution of trajectory ensembles are developed, and these methods have potential computational advantages for the numerical simulation of large quantum systems [27–38]. These approaches are employed to investigate different physical phenomena, such as the quantum tunneling process [27–29,39–41], the photodissociation cross section of the H₂O molecule [42], the autocorrelation function [30,43,44], and entanglement dynamics [45].

*yzheng@sdu.edu.cn

In this paper, we present an alternative trajectory-based formulation to understand the Lévy stable process and Lévy flight dynamics based on the trajectory ensemble propagation of the PDF in phase space. Also, the framework of the trajectory in phase space could be of potential advantage numerically for a multidimensional system. For the Lévy flight, its PDF is described via the fractional FFPE. This leads to the fractional equation of trajectory (FET), namely, we extend the concept of trajectory to the fractional order in phase space. Also, the ensemble of the fractional trajectories has the “interaction” between the fractional trajectories since the distribution of the Lévy flight is of the heavy tail. In a different view, in phase space, we show the flight behaviours of the Lévy flight by employing our fractional trajectories. In addition, we give their vivid physical pictures.

In the following, we describe the theoretical framework of the fractional equations of trajectory in Sec. II. Then, we show the applications of the fractional equations of trajectory for four cases of Lévy processes: the free flight, confined in a quartic potential, escape from a metastable potential and viscous barrier crossing of Lévy types. The discussions and conclusion are given in Sec. IV.

II. THEORETICAL FRAMEWORK

In the probability theory, if a quantity that moves continuously according to a stochastic process, its PDF $W(\Gamma, t)$ could, in the continuity equation, be written as [46]

$$\frac{\partial W(\Gamma, t)}{\partial t} + \nabla \mathbf{j}(\Gamma, t) = 0, \quad (5)$$

where $\mathbf{j}(\Gamma, t)$ is the flux vector, the del operator is the gradient operator, and $\Gamma = (\mathbf{x}, \mathbf{p})$ is the coordinates in phase space. The flux vector and the del operator in phase space are defined as follows:

$$\mathbf{j}(\Gamma, t) = \dot{\Gamma} W(\Gamma, t) \equiv (\dot{\mathbf{x}}, \dot{\mathbf{p}}) W(\Gamma, t), \quad (6)$$

$$\nabla = \left(\frac{\partial}{\partial \mathbf{x}}, \frac{\partial}{\partial \mathbf{p}} \right). \quad (7)$$

For the one-dimensional (1D) case of Eq. (1), the flux $\mathbf{j}(x) = \dot{x} W(x, t)$ and $\nabla = \frac{\partial}{\partial x}$. By comparing the continuity equation of Eqs. (5) and (1), we obtain

$$\begin{aligned} \nabla \mathbf{j}(x) &= \frac{\partial}{\partial x} [\dot{x} W(x, t)] \\ &= -\frac{\partial}{\partial x} [U'(x) W(x, t)] - D \mathcal{D}_x^\alpha W(x, t). \end{aligned} \quad (8)$$

The above equation can also be written as

$$\dot{x} = -U'(x) - \frac{D}{W(x, t)} \mathcal{D}_x^{\alpha-1} W(x, t). \quad (9)$$

Namely, we obtain the equation of trajectory. Since the equation of trajectory of Eq. (9) is related to the fractional derivative of its PDF, we note the equation of trajectory of Eq. (9) as the fractional equation of trajectory (FET).

We can see that Eq. (9) has a similar form with Langevin equation. The difference is the second term depends on PDF and its fractional derivative instead of the noise from the anomalous behavior. This fundamentally different kind of term

leads to an interdependence between the evolving trajectories, that is, there are “interactions” between the trajectories via the term of $\mathcal{D}_x^{\alpha-1} W(x, t)$ in Eq. (9) since the PDF $W(x, t)$ is determined by the ensemble of trajectories [see the following descriptions of Eq. (16)]. This makes the statistical independence of an ensemble representation of the density being broken and the PDF must be propagated as an ensemble.

For the Lévy flight with viscous [9], the FFPE is an extension of the Klein-Kramers equation containing fractional derivatives with respect to momentum. When the diffusion dynamics under the influence of an external potential $U(x)$ and a white Lévy noise, the fractional Klein-Kramers equation of the probability function $W(x, p, t)$ can be written as [21]

$$\begin{aligned} \frac{\partial W(x, p, t)}{\partial t} &= -\frac{p}{m} \frac{\partial W(x, p, t)}{\partial x} + U'(x) \frac{\partial W(x, p, t)}{\partial p} \\ &+ \gamma \frac{\partial [p W(x, p, t)]}{\partial p} + D \mathcal{D}_p^\alpha W(x, p, t), \end{aligned} \quad (10)$$

where γ is the friction constant.

According to the definitions of the flux vector of Eq. (6) and the del operator of Eq. (7) in phase space, we have

$$\begin{aligned} \nabla \mathbf{j}(\Gamma, t) &= \frac{\partial}{\partial x} [\dot{x} W(x, p, t)] + \frac{\partial}{\partial p} [\dot{p} W(x, p, t)] \\ &= \frac{p}{m} \frac{\partial W(x, p, t)}{\partial x} - U'(x) \frac{\partial W(x, p, t)}{\partial p} \\ &- \gamma \frac{\partial [p W(x, p, t)]}{\partial p} - D \mathcal{D}_p^\alpha W(x, p, t). \end{aligned} \quad (11)$$

Equation (11) immediately leads to the following equations:

$$\begin{aligned} \dot{x} &= \frac{p}{m}, \\ \dot{p} &= -U'(x) - \gamma p - \frac{D}{W(x, p, t)} \mathcal{D}_p^{\alpha-1} W(x, p, t). \end{aligned} \quad (12)$$

This is the two-dimensional form of the fractional equation of trajectory (FET) for Lévy flight in phase space.

By employing FET [Eq. (9) for the one-dimensional case and Eq. (20) for the two-dimensional case], we can investigate the Lévy flight dynamics if its PDF $W(x, p, t)$ is known.

We could represent the PDF by employing the ensemble of trajectories based on the theory of Kernel density estimation (KDE) [47]. With the KDE, the PDF can be obtained from a combination of localized functions centered on members of the data set. Namely, the PDF can be written as

$$W(\Gamma, t) = \frac{1}{N} \sum_{i=1}^N \rho[\Gamma - \Gamma_i(t)], \quad (13)$$

where N is the numbers of sampling data or the number of trajectory in our case, $\rho[\Gamma - \Gamma_i(t)]$ is the kernel function in KDE, and $\Gamma_i(t)$ is the position in phase space of the i th trajectory at time t .

In our theoretical framework, the Gaussian kernels are employed in Eq. (13). For the one-dimensional case, it can be written as

$$\rho(x) = \frac{1}{\sqrt{2\pi} h_x \delta_x} \exp\left(-\frac{x^2}{2h_x^2 \delta_x^2}\right), \quad (14)$$

where $h_x > 0$ is the bandwidth which depends on the dimensionality of the data set and the functional form of the kernel. For ℓ -dimensional data sets and Gaussian kernels, $h_x = [4/[N(\ell + 2)]]^{1/(\ell+4)}$ [47]. δ_x is a characteristic length scale of the density function. For Eq. (1), the time-dependent PDF in terms of the trajectory ensemble is then given by

$$W(x,t) = \frac{1}{N} \sum_{j=1}^N \rho[x - x_j(t)]. \quad (15)$$

The initial distributions can be generated by selecting the random variables sampled using the given initial probability distribution or a grid of initial conditions with a local density proportional to the initial probability. Then, with the help of KDE, a smooth function can be constructed. Finally, the ensemble FET of Eq. (9) can be expressed as

$$\dot{x}_i = -U'(x_i) - \frac{D}{W(x_i)} \mathcal{D}_x^{\alpha-1} W(x_i), \quad (16)$$

where the fractional term can be given explicitly by

$$\mathcal{D}_x^{\alpha-1} W(x_i) = \sum_{j=1}^N \left. \frac{\partial^{\alpha-1} \rho[x - x_j(t)]}{\partial |x|^{\alpha-1}} \right|_{x_i}. \quad (17)$$

The interaction between the members of the ensemble is reflected in the last term of Eq. (16).

The calculation of the fractional derivative of the kernel function of Eq. (14) can be obtained analytically by employing Eq. (4) and the Fourier transform. After some algebra, we have

$$\begin{aligned} \mathcal{F}_\alpha(x) &\equiv \mathcal{D}_x^\alpha \rho(x) \\ &= -C_\alpha {}_1F_1\left(\frac{\alpha+1}{2}, \frac{3}{2}; -\frac{x^2}{2\sigma_x^2}\right) \Gamma\left(\frac{\alpha-1}{2}\right) x, \end{aligned} \quad (18)$$

where $C_\alpha = \frac{2^{\frac{\alpha-3}{2}}}{\pi} (\alpha-1) \sigma_x^{-\alpha-1}$ with $\sigma_x = h_x \delta_x$, $\Gamma(\cdot)$ is the Γ function and ${}_1F_1(a,b;z)$ is the Kummer confluent hypergeometric function. $\mathcal{F}_\alpha(x)$ in Eq. (18) can be considered as the kernel of the Riesz fractional derivative and provides a more convenient tool for representing the derivative term in Eq. (17).

Similarly, for the two-dimensional case, the time-dependent PDF in terms of the trajectory ensemble can be written as

$$\begin{aligned} W(x,p,t) &= \frac{1}{N} \sum_{j=1}^N \rho[\Gamma - \Gamma_j(t)] \\ &= \frac{1}{N} \sum_{j=1}^N \rho[x - x_j(t), p - p_j(t)]. \end{aligned} \quad (19)$$

Thus, the ensemble of FET for the two-dimensional case can be written in the following form:

$$\begin{aligned} \dot{x}_i &= \frac{p_i}{m}, \\ \dot{p}_i &= -U'(x_i) - \gamma p_i - \frac{D}{W(x_i, p_i, t)} \mathcal{D}_p^{\alpha-1} W(x_i, p_i, t). \end{aligned} \quad (20)$$

III. NUMERICAL RESULTS AND DISCUSSIONS

In this section we numerically investigate four typical cases for the Lévy flight dynamics. We also discuss the dynamical behaviors of anomalous barrier crossing in phase space.

A. Free Lévy flight

As the simple case we first consider the case of free flight where the potential $U(x) = 0$. The anomalous diffusion equation, for this case, is

$$\frac{\partial W(x,t)}{\partial t} = D \mathcal{D}_x^\alpha W(x,t). \quad (21)$$

The free Lévy flight equation, Eq. (21), can be solved analytically in terms of Fox's H function [10,48] under the initial condition of $W(x,0) = \delta(x)$. With the theoretical framework of the trajectory-based formulation in Sec. II, the ensemble of FET of constituent trajectories can be expressed as

$$\dot{x}_i = -D \frac{\sum_{j=1}^N \mathcal{F}_\alpha[x_i - x_j(t)]}{\sum_{j=1}^N \rho[x_i - x_j(t)]}, \quad (22)$$

where the expressions of $\rho[x_i - x_j(t)]$ and $\mathcal{F}_\alpha[x_i - x_j(t)]$ are given by Eqs. (14) and (18), respectively.

Figure 1 displays the exact numerical results and the results of the trajectory-based formulation of PDFs of free Lévy flight at different times $t = 1, 10$ for $\alpha = 1, 1.5, 2$, respectively. The initial distribution is set as the Gaussian form $W(x,0) = 1/\sqrt{2\pi} \exp(-x^2/2)$ and the diffusion factor $D = 1$. The exact numerical results are obtained by employing FFT. From Fig. 1, it can be seen that the numerical results of FET are in excellent agreement with the exact numerical results.

B. Cauchy-Lévy flight in a quartic potential

An important point in understanding a random process is its behavior in external fields. We now consider the Cauchy-Lévy flight in the quartic potential $U(x) = \frac{1}{4}x^4$. In this case, the stationary spatial distribution is characterized by a bimodality sharp [49]. This peculiarity stems from the long jump's property of the particle in Lévy flight. Driving by Lévy noise, the particle reaches very quickly to the region near the potential wall, then it spends a long time diffusing around until a new long jump in the opposite motion moves it to reach the other side of the potential. This leads to the existence of two wells on both sides of the axis of symmetry. For the typical case of $\alpha = 1$ and $D = 1$, we can obtain the stationary PDF by inverse Fourier transform [50]

$$W_{\text{st}}(x) = \frac{1}{\pi(1 - x^2 + x^4)}. \quad (23)$$

In Fig. 2, we present the results of PDF using the FET for the long time evolution. The initial Gaussian distribution is set as the form $W(x,0) = 2/\sqrt{2\pi} \exp(-2x^2)$. Also, we plot the analytical result of Eq. (23) in the figure. As the figure shows, the agreement between the analytical expression of Eq. (23) and the result of the FET is excellent. This further indicates the accuracy and reliability of the trajectory-based formulation.

C. Escape dynamics from a metastable potential

In this section we investigate the escape dynamics of a particle of Lévy type in a metastable potential. We here use the cubic potential: $U(x) = \frac{1}{2}m\omega^2 x^2 - \frac{1}{3}bx^3$. By employing atomic units, we consider a particle of the mass

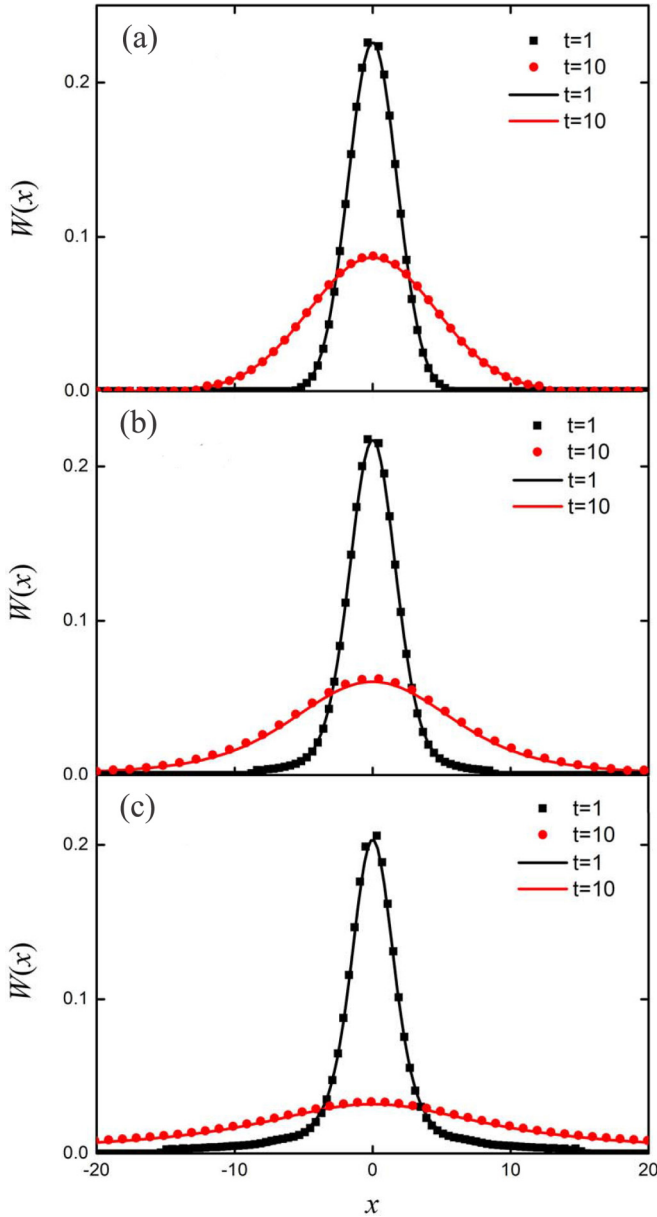


FIG. 1. The PDF with different α values and time. Panel (a) is for $\alpha = 2$, panel (b) is for $\alpha = 1.5$, and panel (c) is for $\alpha = 1$. The exact numerical results are shown in solid lines and the results of trajectory-based formulation are in dots. The solid squares are for time $t = 1$, and the dots are for time $t = 10$. The number of ensemble trajectories is $N = 200$.

$m = 2000$ moves in the potential with $\omega = 0.01$ and $b = 0.2981$. For these parameters, the height of the barrier is $U_h = 0.015$ at $x_h = 0.6709$. Under these parameters, this system can roughly mimic a hydrogen atom bound with approximately two metastable bound states [27]. The characteristic length of the initial Gaussian distribution is set as $\delta_x = \sqrt{\hbar/2m\omega}$, with $\hbar = 1$, and the corresponding central position of $x_0 = -0.2$. In our simulation, the diffusion coefficient is $D = mk_B T = 0.1$, where k_B is the Boltzmann constant and T is the temperature, the minimum of the potential is set as $U_{\min} = -0.015$ for $x > 1.12556$.

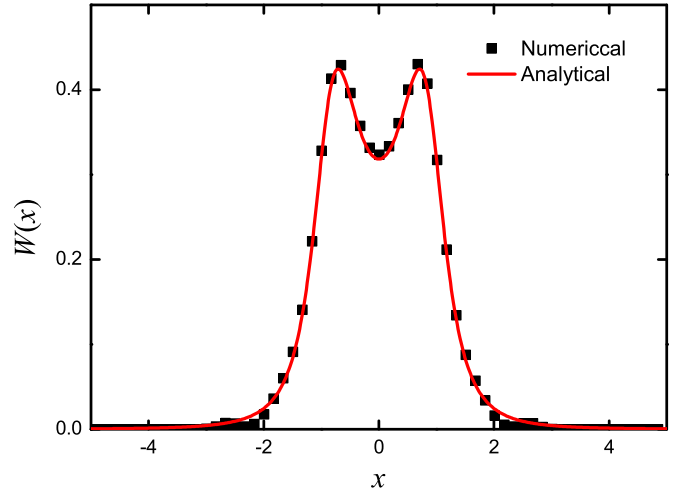


FIG. 2. The stationary PDF of the Cauchy-Lévy flight in a quartic potential. The solid line is the results of Eq. (23), and the solid squares are the results of the trajectory-based formulation using the number of trajectories $N = 200$.

In Fig. 3, we display the time dependence of escape probabilities for several α values. The exact numerical results are obtained using the FFT method. The numerical probabilities of the FET are calculated by counting the number of trajectories that cross the top of the barrier. As shown in the figure, in the large time scale, the agreements between them are perfect. However, there are few distinctions in the short time scale especially for small α values. Since the escape probability is determined by the number of trajectories that have crossed the barrier, the probability can take place only with the first escaping of the trajectories. Thus, the trajectory-based probability may lessen the exact result in short time scales, but they will tend to accordance after the escape of a large numbers of trajectories.

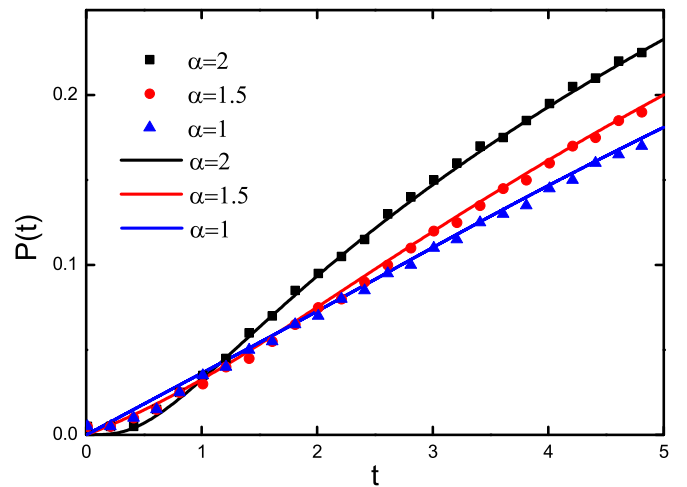


FIG. 3. The escape probabilities of the particle from the metastable potential for several α values. The exact numerical results are in solid lines and the solid squares (for $\alpha = 2$), dots (for $\alpha = 1.5$), and solid triangles (for $\alpha = 1$) are the numerical results of trajectory-based formulation with $N = 200$, respectively.

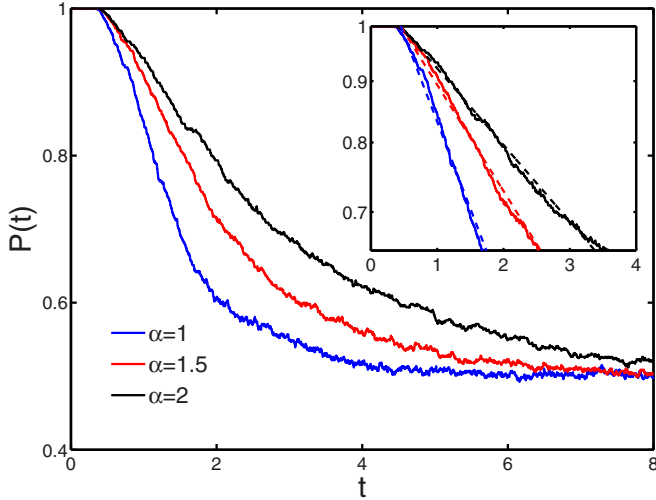


FIG. 4. The survival probabilities of the particle in the left potential well for several α values. The thumbnail presents the decay part of the survival probabilities and dashed lines represent the $\exp[-(t - t_0)/T_w]$ approximation to survival probabilities. The parameters used here are $t_0 = 0.45$ and $T_w = 6.8, 4.9, 3.0$ for $\alpha = 2, 1.5, 1$ (from top to bottom), respectively.

D. Fractional Klein-Kramers equation

In this section we consider the full phase-space barrier crossing in a bistable system which is often used to model chemical reactions, nucleation processes, or the escape of a particle from an external potential of finite height. The potential is defined as $U(x) = 4x^4 - 8x^2$. In the numerical calculations, the scale parameters are preset to $m = 1$ and $\gamma = 1$. The diffusion coefficient of $D = 4$ is equal to the barrier height. The Gaussian distribution of the particle is located at the center of the left well initially. The characteristic lengths of position and momentum are set as $\delta_x = 0.25$ and $\delta_p = 0.25$. In addition, we employ the ensemble of trajectories with $N = 625$ trajectories for this system. The survival probability of the particle in the left well can be calculated via

$$P(t) = \int_{-\infty}^{+\infty} dp \int_{-\infty}^0 dx W(x, p, t). \tag{24}$$

Figure 4 shows the time dependence of survival probabilities for several α values. It is seen that the smaller the value of α , the greater the escaping rate. This stems from the long-jump properties of a particle undergoing Lévy flight, which causes the divergence characteristics of the mean kinetic energy. As shown in the inset of the figure, the thumbnail part displays the most decayed part of the survival probabilities. The dashed lines are plotted using $P_e(t) = \exp[-(t - t_0)/T_w]$, where t_0 and T_w stand for the initial decay time and the mean waiting time, respectively. As it shows, the survival probabilities decay exponentially which are in consistent with the conclusions in Ref. [51].

To analyze further the characteristic behaviors of the barrier crossing problem of Lévy types, in Fig. 5 we plot the evolution graph of four typical cases of trajectories in phase space for several α values. As shown in Fig. 5(a), all of the trajectories have finished the crossing processes, but their speeds increase with the decrease of α when they reach the top of the barrier.

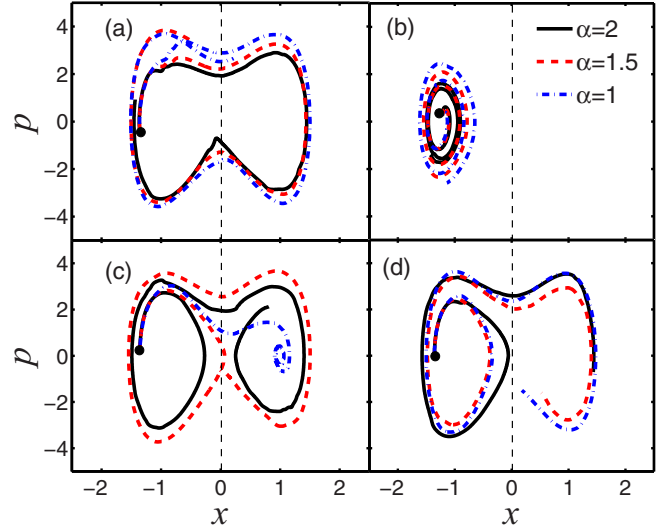


FIG. 5. Four typical phase-space behaviors of several trajectories. The dashed line and the black solid circle stand for the position of the barrier of the double well potential and the initial position of the trajectory, respectively.

That is, if the trajectory in normal diffusion goes over the barrier by walk then the one in Lévy flight overpasses by flight. In addition, in the same evolution time, the trajectory with smaller α value will move further. This is due to the long tail characteristics of the PDF of Lévy flight. In Fig. 5(b), we show a different case: all the trajectories rotate spirally with the exception of $\alpha = 1$, which spreads more broadly. Figure 5(c) displays another important property of the Lévy flight trajectory. For the case of $\alpha = 1$, the trajectory crosses the barrier directly but it rapidly gets trapped in the bottom of the left potential well. This can be attributed to the sharp peak property of the PDF of Lévy flight, and with more trajectories getting trapped in the bottom it can prevent the peak from being sharp enough. In Fig. 5(d) we present the case that, although the trajectory in normal diffusion crosses the barrier with highest speed, the route of the normal trajectory is still the shortest one compared to the Lévy flight cases.

IV. CONCLUSION

In this paper, we present a new trajectory-based formulation for Lévy flight dynamics. By employing the theory of Kernel density estimation (KDE) with the Gaussian kernel of PDF we derive the fractional equation of trajectory (FET), and a new kernel in terms of the confluent hypergeometric function is derived to represent the fractional Riesz fractional derivative. Numerical simulations are carried out for free Lévy flight, Lévy flight in a quartic potential, and the escape problem of Lévy types employing FET; all of the results of FET are in excellent agreement with the exact results. In addition, we investigate the full phase-space barrier crossing of Lévy types by employing the trajectory-based formulation, or the fractional equation of trajectory in phase space. It is shown that the survival probability decays proximate exponentially and the decay rate increases quickly with the decrease of α . This is

consistent with the characteristic of a Lévy motion occurring on a confined interval between two absorbing boundaries [52]. In phase space, by observing the motions of the trajectories, the features of Lévy flight are interpreted vividly.

Recently, a measurement of the phase-space density distribution (PSDD) of ultra-cold ^{87}Rb atoms performing 1D anomalous diffusion was shown [53]. It was shown that the position-velocity correlation function $C_{xv}(t)$, obtained from the PSDD, decays asymptotically as a function of time with a power law. Based on our theoretical framework, we can investigate this dynamical anomalous correlation in phase space to present their dynamical behaviors of anomalous diffusion and the power-law asymptotic dynamics of the position and velocity. Also, by following the dynamical evolution of the trajectory, we could glance at the anomalous behaviors.

It is correct that the method works only within a certain amount of time and within a finite spatial domain, but by increasing the number of trajectories, we can increase the accuracy. Future work can deal with the proposition of the replacement of the Gaussian kernel with the adaptive kernel, which might increase the level of accuracy of the method.

ACKNOWLEDGMENTS

This work was supported by the National Science Foundation of China (Grant No. 11674196) and the National Basic Research Program of China (973 Program, Grant No. 2015CB921004). Z.S. also gratefully acknowledges partial support from the National Science Foundation of China of No. 11704173.

-
- [1] J. Klafter, A. Blumen, and M. F. Shlesinger, *Phys. Rev. A* **35**, 3081 (1987).
- [2] V. Zaburdaev, S. Denisov, and J. Klafter, *Rev. Mod. Phys.* **87**, 483 (2015).
- [3] D. Xiong, *Europhys. Lett.* **113**, 14002 (2016).
- [4] D. A. Kessler and E. Barkai, *Phys. Rev. Lett.* **105**, 120602 (2010).
- [5] E. Barkai, E. Aghion, and D. A. Kessler, *Phys. Rev. X* **4**, 021036 (2014).
- [6] B. B. Mandelbrot and J. W. van Ness, *SIAM. Rev.* **10**, 422 (1968).
- [7] K. M. Kolwankar and A. D. Gangal, *Phys. Rev. Lett.* **80**, 214 (1998).
- [8] R. Metzler, E. Barkai, and J. Klafter, *Phys. Rev. Lett.* **82**, 3563 (1999).
- [9] E. Lutz, *Phys. Rev. Lett.* **86**, 2208 (2001).
- [10] S. Jespersen, R. Metzler, and H. C. Fogedby, *Phys. Rev. E* **59**, 2736 (1999).
- [11] A. Ott, J. P. Bouchaud, D. Langevin, and W. Urbach, *Phys. Rev. Lett.* **65**, 2201 (1990).
- [12] H. Katori, S. Schlipf, and H. Walther, *Phys. Rev. Lett.* **79**, 2221 (1997).
- [13] G. Zumofen and J. Klafter, *Phys. Rev. E* **51**, 2805 (1995).
- [14] G. M. Viswanathan, V. Afanasyev, S. V. Buldyrev, E. J. Murphy, P. A. Prince, and H. E. Stanley, *Nature (London)* **381**, 413 (1996).
- [15] N. E. Humphries, H. Weimerskirch, N. Queiroz, E. J. Southall, and D. W. Sims, *Proc. Natl. Acad. Sci. U.S.A.* **109**, 7169 (2012).
- [16] H. C. Fogedby, *Phys. Rev. E* **58**, 1690 (1998).
- [17] H. C. Fogedby, *Phys. Rev. Lett.* **73**, 2517 (1994).
- [18] R. Metzler, E. Barkai, and J. Klafter, *Europhys. Lett.* **46**, 431 (1999).
- [19] C. Celik and M. Duman, *J. Comput. Phys.* **231**, 1743 (2012).
- [20] S. G. Samko, A. A. Kilbas, and O. I. Marichev, *Fractional Integrals and Derivatives—Theory and Applications* (Gordon and Breach, New York, 1993).
- [21] R. Metzler and J. Klafter, *J. Phys. Chem. B* **104**, 3851 (2000).
- [22] M. Ciesielski and J. Leszczynski, *arXiv:math/0506556* (2005).
- [23] C. Li, W. Deng, and Y. Wu, *Numer. Meth. Part. D. E.* **28**, 1944 (2012).
- [24] F. Liu, P. Zhuang, I. Turner, K. Burrage, and V. Anh, *Comput. Math. Appl.* **59**, 1718 (2010).
- [25] C. P. Li, Z. G. Zhao, and Y. Q. Chen, *Comput. Math. Appl.* **62**, 855 (2011).
- [26] B. J. West, *Rev. Mod. Phys.* **86**, 1169 (2014).
- [27] A. Donoso and C. C. Martens, *Phys. Rev. Lett.* **87**, 223202 (2001).
- [28] A. Wang, Y. Zheng, C. C. Martens, and W. Ren, *Phys. Chem. Chem. Phys.* **11**, 1588 (2009).
- [29] X. Zhang and Y. Zheng, *Chin. Phys. Lett.* **26**, 023404 (2009).
- [30] E. J. Heller, *J. Chem. Phys.* **62**, 1544 (1975).
- [31] T. Dittrich, C. Viviescas, and L. Sandoval, *Phys. Rev. Lett.* **96**, 070403 (2006).
- [32] P. P. de M Rios and A. M. O. D. Almeida, *J. Phys. A* **35**, 2609 (2002).
- [33] A. Donoso and C. C. Martens, *J. Chem. Phys.* **116**, 10598 (2002).
- [34] A. Shimshovitz and D. J. Tannor, *Phys. Rev. Lett.* **109**, 070402 (2012).
- [35] J. Cerrillo and J. Cao, *Phys. Rev. Lett.* **112**, 110401 (2014).
- [36] Y. Chen, J. Q. You, and T. Yu, *Phys. Rev. A* **90**, 052104 (2014).
- [37] R. E. Wyatt, *Quantum Dynamics with Trajectories* (Springer, New York, 2005).
- [38] *Quantum Trajectories*, edited by P. K. Chattaraj, (CRC, Boca Raton, FL, 2010).
- [39] L. Wang, C. C. Martens, and Y. Zheng, *J. Chem. Phys.* **137**, 034113 (2012).
- [40] F. Xu and Y. Zheng, *Acta. Phys. Sin.* **62**, 213401 (2013).
- [41] H. Li, J. Poulsen, and G. Nyman, *J. Phys. Chem. Lett.* **4**, 3013 (2013).
- [42] F. Xu, L. Wang, C. C. Martens, and Y. Zheng, *J. Chem. Phys.* **138**, 024103 (2013).
- [43] J. Liu and W. H. Miller, *J. Chem. Phys.* **126**, 234110 (2007).
- [44] L. Wang and Y. Zheng, *Chem. Phys. Lett.* **563**, 112 (2013).
- [45] F. Xu, C. C. Martens, and Y. Zheng, *Phys. Rev. A* **96**, 022138 (2017).
- [46] D. A. McQuarrie, *Statistical Mechanics* (Harper Collins, New York, 1976).
- [47] B. W. Silverman, *Density Estimation for Statistics and Data Analysis* (Chapman and Hall, London, 1986).

- [48] B. J. West, P. Grigolini, R. Metzler, and T. F. Nonnenmacher, [Phys. Rev. E **55**, 99 \(1997\)](#).
- [49] A. V. Chechkin, J. Klafter, V. Y. Gonchar, R. Metzler, and L. V. Tanatarov, [Phys. Rev. E **67**, 010102 \(2003\)](#).
- [50] J. Klafter and I. M. Sokolov, *First Steps in Random Walks* (Oxford University Press, London, 2011).
- [51] P. D. Ditlevsen, [Phys. Rev. E **60**, 172 \(1999\)](#).
- [52] B. Dybiec, E. Gudowska-Nowak, E. Barkai, and A. A. Dubkov, [Phys. Rev. E **95**, 052102 \(2017\)](#).
- [53] G. Afek, J. Coslovsky, A. Courvoisier, O. Livneh, and N. Davidson, [Phys. Rev. Lett. **119**, 060602 \(2017\)](#).